FORSCHUNGSZENTRUM
ROSSENDORF e.V.

FZR

FZR-91
Juni 1995
Preprint

E.E. Kolomeitsev, D.N. Voskresensky and B. Kämpfer

The impact of kaon polarization in nuclear matter on the K^- production in heavy-ion collisions

Forschungszentrum Rossendorf e.V.
Postfach 51 01 19 · D-01314 Dresden
Bundesrepublik Deutschland

Telefon (0351) 591 3258
Telefax (0351) 591 3700
E-Mail kaempfer@fz-rossendorf.de

The impact of kaon polarization in nuclear matter on the K^- production in heavy-ion collisions

E.E. KOLOMEITSEV[a,b], D.N. VOSKRESENSKY[c,1], B. KÄMPFER[a,b]

[a] *Institut für Kern- und Hadronenphysik, Forschungszentrum Rossendorf e.V., PF 510119, D-01314 Dresden, Germany*

[b] *Institut für Theoretische Physik, TU Dresden, Mommsenstr. 13, D-01062 Dresden, Germany*

[c] *Gesellschaft für Schwerionenforschung, PF 110552, D-64220 Darmstadt, Germany*

Abstract

The impact of the kaon polarization in nuclear matter on the K^- yield in intermediate-energy heavy-ion collisions is investigated. Our scenario of the strange particle production and dynamics is based on an expanding fireball model. This allows for a proper account of in-medium effects. A relation between observed K^+ and K^- yields is derived. Differential K^- cross sections are calculated and compared with available experimental data taken at various collision energies. It turns out that in-medium effects can modify the K^- yields by factors 2 to 5 at beam energies between 2 and 1 AGeV.

1 Introduction

In the field of heavy-ion collisions (HIC) such particles are of particular interest, which are not present in the entrance channel. It is generally thought that these particles represent sensitive messengers from the hot and dense reaction zone. Among the experimentally feasible particles are the strangeness carrying particles. These ones are comparatively heavy so that one might expect that their production can serve as useful probe of cooperative effects of the heavy-ion collision dynamics.

The advent of experimental information on the total K^- meson yields and momentum spectra in HIC at intermediate energies [1, 2, 3, 4, 5] stimulates further theoretical investigations of this special strange channel [6, 7]. In the intermediate energy region the strange particle production proceeds via subthreshold or nearly threshold mechanisms. Therefore, possible in-medium effects seem to be important. However, even the elaborated dynamical schemes do not yet allow for a proper inclusion of the genuine in-medium effects. Having been touched, e.g. in refs. [7, 8, 9], this complicated problem remains not fully solved.

[1] Permanent address: Moscow Engineering Physical Institute, Kashirskoe shosse 31, 115409 Moscow, Russia

In this paper we are going to investigate a possible influence of the kaon polarization in nuclear matter on the dynamics and the yield of the negatively strange particles in the course of HIC. First, we shall present a scenario of HIC, which despite of a simplified treatment of the collision dynamics, allows for a proper account of the in-medium effects. Then we shall demonstrate how the kaon polarization in nuclear matter affects the observable K^- yield.

We restrict ourselves to the consideration of beam energies $E_{lab} \lesssim 2$ AGeV achieved at the LBL Bevalac and GSI SIS facilities. The gross properties HIC at such energies can be described fairly well within an expanding fireball model [10, 11, 12], which is appropriate to include the in-medium effects, in particular, the changes of the BB ($B = N, \Delta$) and πB interactions in nuclear matter (see refs. [13, 14, 15, 16, 17, 18] and further references therein).

In applying this model we suppose that the energy in the center-of-mass system of a nucleus-nucleus collision, contained within the overlap region of colliding nuclei, is spent on the creation of a quasi-equilibrium nuclear system (i.e., the fireball) characterized by some initial temperature T_m and density ρ_m. These values are determined in refs. [13, 18] by the equation of state of nuclear matter and the initial collision energy per nucleon in the center-of-mass system $E_{c.m.}$. Assuming entropy conservation we find the dependence of the temperature on the density, $T(\rho)$, during the quasi-equilibrium expansion stage. This expansion lasts for a certain time $0 < t \lesssim t_o$ up to a breakup stage, when the fireball density becomes rather low and the inter-particle collisions are so rare that the particle momentum distributions freeze out. The transition to the free-stream stage occurs within some time interval $t_o - \tau_b/2 < t < t_o + \tau_b/2$, while the particles evolve from in-medium states to the vacuum state. For the nucleons and pions the transition from the quasi-equilibrium momentum distributions of the in-medium quasi-particles to the free particle distributions can be considered as rather fast. The breakup density is estimated within our model as $\rho_b \sim 0.6 - 0.7\rho_o$, where $\rho_o = 0.17$ fm^{-3} is the nuclear saturation density. It is supported qualitatively by estimates of the pion and nucleon mean free paths [14]. The corresponding breakup temperature is unambiguously expressed through $E_{c.m.}$ and ρ_b (and $T_b = T(\rho_b, E_{c.m.})$).

Relying on these assumptions the differential cross sections can be calculated with a proper inclusion of in-medium effects [13, 15, 16, 17, 18]. Although simple, this model is in general confirmed by the agreement of the calculated differential cross sections of the pion, nucleon and photon production with available experimental data for various bombarding energies and colliding nuclei. Below we use the functions $T(t)$ and $\rho(t)$ and the values T_m, ρ_m, T_b and ρ_b from these previous calculations [13, 15, 16, 17, 18].

Our papers is organized as follows. In section 2 we supplement the fireball model by a scenario for the strange particle production. The main peculiarities of the kaon polarization in nuclear matter we describe shortly in section 3. The relation between the chemical potential of K^- mesons and the number of K^+ mesons produced in the collision is established in section 4. The fireball breakup processes is considered in section 5. In section 6 we compare our model calculations with the available experimental data and find good agreement when utilizing the correct in-medium properties of kaons. Our

conclusions are summarized in section 7.

2 A scenario for strange particle dynamics

In order to include the strangeness degree of freedom into our considerations the above mentioned fireball model needs to be supplemented by a scenario for the strange particle production.

The temperatures and densities reached in HIC, at the beam energies under consideration, are estimated as $T \lesssim m_\pi$, where $m_\pi \simeq 139$ MeV is the pion mass, and $\rho \lesssim 3\rho_o$. The most frequent strange particles created in such collisions are K^+, K^o and K^-, $\bar{K}^o$ mesons, and Λ and Σ hyperons. The admixture of the heavy double-strange particles, the heavier strange meson and hyperon resonances as well as the anti-hyperons is considerably smaller.

Having the strangeness $S = -1$, the K^-, $\bar{K}^o$ mesons and Λ, Σ hyperons are produced in strong interaction processes only in association with K^+, K^o mesons ($S_{K^+} = S_{K^o} = 1$):

$$BB \longrightarrow K^{+,o}YB, \quad \pi N \longrightarrow K^{+,o}Y, \quad Y = \Lambda(\Sigma) \tag{1}$$

and

$$BB \longrightarrow K^{-,\bar{o}}K^{+,o}BB, \quad \pi\pi \longrightarrow K^{-,\bar{o}}K^{+,o}, \tag{2}$$

where B stands for the nucleons and the nucleon resonances, and π denotes the pion of appropriate charge. The thresholds of these direct reactions in the $N - N$ channel are rather high: $E_{th} \simeq m_K + m_\Lambda - m_N \simeq 4.8m_\pi$ for reactions (1) and $E_{th} \simeq 2m_K \simeq 7m_\pi$ for reactions (2), i.e., the production proceeds via cooperative subthreshold mechanisms, which can be described microscopically as multistep reactions. Therefore, in HIC at beam energies $E_{lab} \lesssim 2$ AGeV strange particles are, in general, produced predominantly in the initial stage of the collision, which in our simplified quasi-equilibrium model corresponds to the temperature and the density nearby their maximum values T_m and ρ_m.

The particles of distinct strangeness interact differently with the nuclear environment, e.g., the positively strange particles K^+, K^o have essentially longer mean free paths than the negatively strange particles K^-, $\bar{K}^o$, Λ, Σ. The mean free paths of K^+ and K^- mesons, λ_{K^+} and λ_{K^-} respectively, can be roughly estimated by using the free kaon-nucleon cross sections $\sigma_{K^+N} \simeq 10$ mb and $\sigma_{K^-N} \simeq 40$ mb. Then we have $\lambda_{K^+} \simeq 1/\sigma_{K^+N}\rho \simeq 2$ fm for $\rho = 3\rho_o$ (about maximum density) and $\lambda_{K^+} \simeq 12$ fm for $\rho = 0.5\rho_o$ (about breakup density), whereas $\lambda_{K^-} \simeq 1/\sigma_{K^-N}\rho \simeq 0.5$ fm for $\rho = 3\rho_o$ and $\lambda_{K^-} \simeq 3$ fm for $\rho = 0.5\rho_o$. These estimates support the statement that $\lambda_{K^+} \gg \lambda_{K^-}$, which also coincides with microscopical calculations [19, 20]. By the reason of isotopical symmetry analogous estimates are also valid for the K^o and $\bar{K}^o$ mesons, i.e., $\lambda_{K^o} \gg \lambda_{\bar{K}^o}$. Although the probabilities of the rescattering reactions and the corresponding kaon mean free paths are sensitive to the in-medium effects in the baryon-baryon interaction and in the pion dispersion relation [18], we suppose here that proper calculations, which include also the

enrichment of baryon resonances [21] will not change substantially the above estimate $\lambda_{K^+,K^o} \gg \lambda_{K^-,\bar{K}^o}$.

Thus, estimates of the kaon mean free paths as well as the microscopical dynamical calculations provide a support for a strangeness separation during the course of HIC: Due to the long mean free paths the K^+, K^o mesons, having been created in the reactions (1) and (2), can escape from the fireball at a somewhat earlier stage of the collision, i.e., at higher density and temperature. (This leak out of less rescattering particles can be described by drain terms [22].) According to estimates in ref. [17], this stage lasts probably a rather short time $t \sim \tau_{S+}$ of a few fm/c, since the K^+, K^o production rate drops substantially with decreasing temperature and density. Indeed such a saturation of the K^+ production is supported by recent microscopic calculations (see fig. 2 in ref. [9]). On the other hand the negatively strange particles (K^-, $\bar{K}^o$, Λ, Σ) are still confined in the fireball interior during an essentially longer stage $\tau_{S+} < t < t_o$, up to the fireball breakup. Since weak processes do not occur on the time scale $t_o \sim 10$ fm/c, typical for the fireball expansion, the total negative strangeness, confined inside the fireball, accumulates for the time $0 < t < \tau_{S+}$ and remains fixed for the time $t > \tau_{S+}$. (Notice that this scenario resembles somewhat the strangeness distillation process of ref. [23].) During the latter time interval the remaining strangeness is redistributed among the in-medium strange particle states in accordance with the detailed balance equations in the secondary reactions

$$K^{-,\bar{o}}N \leftrightarrow \pi Y, \quad K^{-,\bar{o}}N \leftrightarrow K^{-,\bar{o}}N, \quad N\Lambda \leftrightarrow N\Sigma. \tag{3}$$

For simplicity we assume that the momentum distributions of the negatively strange particles freeze out at approximately the same rather short stage of the collision as the nucleon and the pion distributions do. This assumption allows us to calculate the negatively strange particle yields with an explicit inclusion of in-medium effects. Further we confirm this scenario by calculations and by the found agreement with the available experimental data.

3 Kaon polarization in nuclear matter

Here we consider isotopically symmetrical nuclear matter. The K^- and $\bar{K}^o$ mesons as well as the K^+ and K^o mesons have the same properties in such a nuclear matter. For the description of the K^- meson dispersion we use the results of the recent work [24], where the kaon polarization operator has been calculated by taking into account (i) the s-wave part fitted to the on-shell KN scattering data in ref. [25], (ii) the p-wave part determined by the hyperon (Λ, Σ) - nucleon-hole loops, (iii) the graphs with pionic intermediate states and (iv) the kaon fluctuations. A possible residual off-shell kaon-nucleon interaction has been evaluated with the help of the Adler consistency condition.

The p-wave KN interaction results in the appearance of the two additional branches, $\omega_\Lambda(k)$ and $\omega_\Sigma(k)$, in the K^- and $\bar{K}^o$ excitation spectra in isosymmetrical nuclear matter, which are related to the mixed states of the $\Lambda(\Sigma)$ - nucleon-holes with the quantum numbers of K^- and $\bar{K}^o$ mesons. It was argued in ref. [24] that due to the weakness of

$KN\Sigma$ coupling the Σ branch is only weakly populated by the K^-, $\bar{K}^\circ$ mesons. Therefore, we can omit it in the subsequent considerations.

Although the processes with the pionic intermediate states and the kaon fluctuations are found to be essential at non-vanishing temperatures in the vicinity of the critical point of a possible pion and kaon condensations, their contributions are not as significant at the temperatures and densities reached in intermediate-energy HIC.

Therefore, focusing on a possible qualitative manifestation of the new peculiarities of the kaon in-medium polarization in the observed K^- yields, we shall utilize a simplified version of the kaon polarization operator [24], which includes both the s-wave interaction [7, 25], now constrained by Adler's consistency condition, and the p-wave $KN\Lambda$ interaction. The resulting retarded kaon Green's function $\mathcal{D}^R_{K^-}(\omega, k)$, which depends on frequency ω and momentum k, is given by

$$\left[\mathcal{D}^R_{K^-}(\omega,k)\right]^{-1} = \omega^2 - k^2 - m_K^2 - \Pi_S(\omega,k) - \Pi_A(\omega,k) - \Pi_P(\omega,k), \tag{4}$$

where the pieces of the polarization operator are approximated by

$$\begin{aligned}
\Pi_S(\omega,k) &= -d\, m_K^2 \frac{\rho}{\rho_\circ} - \frac{3}{2}\alpha\,\omega\,\frac{\rho}{\rho_\circ}, \\
\Pi_A(\omega,k) &= -2\,d\,(\omega^2 - k^2 - m_K^2)\,\frac{\rho}{\rho_o}, \\
\Pi_P(\omega,k) &= \frac{1}{2}\frac{A_\circ k^2}{\omega - \tilde{\omega}_\Lambda - \dfrac{k^2-\omega^2}{2m_N^*(\rho)}}\frac{\rho}{\rho_o},
\end{aligned}$$

$$d = \frac{\Sigma_{KN}}{f^2 m_K^2}\rho_\circ, \quad \alpha = \frac{\rho_o}{2f^2}, \quad A_\circ \simeq 1.1 m_\pi, \quad \tilde{\omega}_\Lambda \simeq 1.4 m_\pi,$$

$\hbar = c = 1$, and $m_K = 3.5 m_\pi$ is the kaon mass. The value $m_N^*(\rho)$ is an effective in-medium nucleon mass, e.g., given by the modified Walecka model ($m_N^*(\rho_o) \simeq 0.85 m_N$ at $T = 0$ [26]). It does not significantly depend on the temperature at $T \lesssim m_\pi$ [13]. The value f is assumed to be equal to the pion decay constant $f_\pi \simeq 93$ MeV, and Σ_{KN} is the kaon sigma term. With the choice $\Sigma_{KN} \simeq 2m_\pi$, advocated in several studies [7, 25], we have $d \simeq 0.18$ and $\alpha \simeq 0.57 m_\pi$.

The term Π_S in eq. (4) is essentially the same as that considered in ref. [7] for the K^- polarization operator. It is related to a local $KKNN$ interaction with scalar and vector couplings. The term Π_A in eq. (4) is fixed by the Adler consistency condition and contains some residual off-shell KN interaction [24]. Its inclusion modifies essentially the resulting kaon polarization operator at densities $\rho > \rho_0$ but it is not so important at the rather low breakup densities $\rho \simeq 0.6 - 0.7\rho_0$. The p-wave term Π_P is given by the Λ-particle–proton-hole loop. Such an interaction leads to the appearance of the low-lying Λ branch in the kaon spectrum in nuclear matter which is somehow populated by in-medium $K^-(\bar{K}^\circ)$ mesons. As we shall see the occupation of this branch by the kaons may manifest itself in the kaon production in HIC.

We also note here that the expression (4) depends only on the independent thermodynamical variable ρ, and within our approximations it does not depend longer on the temperature.

The spectrum of $K^-(\bar{K}^o)$ mesons for two densities $\rho = \rho_b \simeq 0.6\rho_o$ and $\rho = 3\rho_o$ is displayed in Fig. 1a. The K^+ (K^o) branches are not shown. For $\rho \to 0$ the upper branch of K^- excitations $\omega_K(k)$ turns into the free (i.e. vacuum) spectrum, $\omega_k = \sqrt{m_K^2 + k^2}$, while the low-lying $\omega_\Lambda(k)$ branch becomes $\sqrt{m_\Lambda^2 + k^2} - m_N$. One observes at breakup density a moderate in-medium modification of the upper branch in Fig. 1a; the essential in-medium effect is the appearance of the second branch.

The factors

$$\Gamma_i(k) = \frac{2\omega_k}{\left(2\omega - \frac{\partial \Pi}{\partial \omega}\right)|_{\omega=\omega_i(k)}}, \; i = K, \Lambda, \tag{5}$$

displayed in Fig. 1b, demonstrate how the in-medium branches of $K^-(\bar{K}^o)$ excitations are occupied by the free kaons (see eq. (14) and discussion below). One observes that the kaons mainly occupy the upper branch, whereas the low-lying branch is more weakly populated by the kaons. The occupation of the low-lying branch by the kaons is increased with increasing density, while the occupation of the upper branch is decreased.

We have also to note that the kaon Green's function given by eq. (4) does not satisfy the sum rule $\int_0^\infty 2\omega Im\mathcal{D}^R d\omega/\pi = 1$ [27]. This means that the kaons are also additionally distributed among virtual kaons and high-lying baryon resonances not taken into account in eq. (4) explicitly. We suppose that all these states are characterized by rather high frequencies, which are not noticeably excited at temperatures of our interest. Thus, such extra kaon degrees of freedom do not affect our resulting kaon distributions.

4 Chemical equilibrium of strange particles

Now let us consider how the total negative strangeness S_- accumulated in the reactions (1, 2) is redistributed among the K^-, $\bar{K}^o$, Λ, Σ quasi-particles via the reactions (3). Making use of the detailed balance for the reactions (3) we can determine the densities of the strange quasi-particles at given values ρ and T by fixing the chemical potential of kaons $\mu_{K^-} = \mu_{\bar{K}^o} \equiv \mu_K$. Since the number of kaons and hyperons is rather small, one can neglect the difference of the Boltzmann, Bose and Fermi statistics. For the $K^-(\bar{K}^o)$ meson density we have in Boltzmann approximation

$$\rho_K(\rho, T) = \rho_{K^-} = \rho_{\bar{K}^o} = \sum_{i=1}^{2} \int \frac{d^3k}{(2\pi)^3} \tilde{\Gamma}_i(k) \exp\left(-\frac{\omega_i(k)}{T} + \frac{\mu_K}{T}\right). \tag{6}$$

Here the summation is to be taken over both in-medium branches of the K^-, $\bar{K}^o$ spectra. The factor $\tilde{\Gamma}_i(k) = \Gamma_i(k)\omega_i(k)/\sqrt{m_K^2 + k^2}$ reflects the redistribution of the kaon quasi-particles between the excitation branches $\omega_K(k)$ and $\omega_\Lambda(k)$.

The $\Lambda(\Sigma)$ density is given by

$$\rho_{\Lambda(\Sigma)}(\rho,T) \approx g_{\Lambda(\Sigma)} \int \frac{2d^3p}{(2\pi)^3} \Gamma_{\Lambda(\Sigma)}(p) \exp\left(-\frac{\sqrt{m^{*2}_{\Lambda(\Sigma)}+p^2}}{T}+\frac{\mu_N+\mu_K}{T}\right), \quad (7)$$

$$\Gamma_{\Lambda(\Sigma)}(p) = \left(1-\frac{\partial\Sigma_{\Lambda(\Sigma)}(\varepsilon_{\Lambda(\Sigma)},p)}{\partial\varepsilon_{\Lambda(\Sigma)}(p)}\right)^{-1},$$

where $g_{\Lambda(\Sigma)} = 1(3)$ is related to the isospin of $\Lambda(\Sigma)$, and $m^*_{\Lambda(\Sigma)}$ denotes the effective mass of Λ and Σ hyperons, and μ_N is the nucleon chemical potential in the medium [16]. Here we assume also that the hyperon masses scale down proportionally to the nucleon mass, i.e. $m^*_{\Lambda(\Sigma)}(\rho) = m_{\Lambda(\Sigma)} + \alpha_S(m^*_N(\rho) - m_N)$ with $\alpha_S = 1$, see ref. [28]. We also for simplicity neglect the retardation effects discussed in ref. [16] in the corresponding hyperon self-energies $\Sigma_Y(\varepsilon_Y, p)$, i.e., we suppose $\partial\Sigma_Y/\partial\varepsilon_Y = 0$ and $\Gamma_{\Lambda(\Sigma)} = 1$.

The relative weights of each strange species (Λ, Σ, K) in the total strangeness S_- are defined by the relations

$$c_K(t) = \frac{\rho_K(\rho(t),T(t))}{S_-/V(t)}, \quad c_{\Lambda(\Sigma)}(t) = \frac{\rho_{\Lambda(\Sigma)}(\rho(t),T(t))}{S_-/V(t)}, \quad (8)$$

which do not depend on the kaon chemical potential. According to the hydrodynamical model [17, 29] the time dependence of the density and the temperature is given by

$$T(t) = \frac{T_m}{\frac{t^2}{t_o^2}\left(\frac{T_m}{T_b}-1\right)+1}, \quad (9)$$

$$\rho(t) = \frac{\rho_m}{\left[\frac{t^2}{t_o^2}\left(\left(\frac{\rho_m}{\rho_b}\right)^{2/3}-1\right)+1\right]^{3/2}}$$

in the interval $0 < t < t_o$.

The functions (8) are plotted in Fig. 2 at fixed laboratory energy in comparison with those values obtained with the free spectra of strange particles. As we can see, the in-medium KN interaction manifests itself through a pronounced enhancement by a factor 2-3 of the effective K^-, $\bar{K}^o$ meson degrees of freedom. Fig. 2 shows that during the fireball's lifetime the created strangeness is mainly stored in the hadron states (Λ and Σ particles). Indeed the fugacity of the $\Lambda(\Sigma)$ particles can be estimated as $g_{\Lambda(\Sigma)}\exp(-[m_{\Lambda(\Sigma)} - m_N + \delta\mu_N + \mu_K]/T)$ (here $\delta\mu_N = \mu_N - m_N$ is the nucleon chemical potential calculated from the nucleon mass). It is lower than the kaon fugacity, which is roughly $\Gamma_i(k)\exp(-[\omega_i(k = 0) + \mu_K]/T)$. The contribution of the Σ particle is also raised by the additional isotopical factor $g_\Sigma = 3$.

The relation between the chemical potential of K^- and the total number of K^+ mesons, N_{K^+}, produced in the collision is given by

$$V(t)\left[2\rho_K(\rho(t),T(t)) + \rho_\Lambda(\rho(t),T(t)) + \rho_\Sigma(\rho(t),T(t))\right] = S_- \approx N_{K^+} + N_{K^o} \approx 2N_{K^+}, \quad (10)$$

where $V(t)$ is the fireball volume at given time and the factor 2 in the left-hand side takes into account the contribution of $\bar{K}^o$ mesons.

The proper calculation of the value N_{K^+} is a separate complicated problem, which has to be worked out by taking into account possible in-medium effects. In this work we shall not calculate this quantity but simply extract it from available experimental data

$$\frac{N_{K^+}}{V(t)} \approx \frac{\sigma_{K^+}(A, E_{lab})}{\sigma_{geom} V(t)},$$

where

$$\sigma_{geom} V = 2\pi \int_0^{b_{max}} db\, b\, V(b) \simeq 2\pi r_o^2 A^{5/3} \rho^{-1}, \tag{11}$$

and $b_{max} = 2 \cdot 1.1 A^{1/3}$ fm stands for the maximum impact parameter of the collision. The quantity $V(b) = 2A/\rho F(b/b_{max})$ is the available fireball volume for the inclusive processes [13] ($F(x)$ is normalized by $\int_0^1 F(x)dx = 1/8$). The value $\sigma_{K^+}(A, E_{lab})$ is the angle integrated K^+ production cross section in $A + A$ reactions at given bombarding energy E_{lab}; according to the model [17] it scales as $\sigma_{K^+}(A) \sim t_o \sigma_{geom} V_m \sim A^2$.

Knowing the experimental dependence $N_{K^+}(E_{lab}, A)$ and also using the functions $T(t_o, E_{lab})$ and $\rho(t_o, E_{lab})$ from refs. [13, 18] one can determine the dependence $\mu(t_o, E_{lab})$. Unfortunately up to now the K^+ yields have been measured only for few nuclei and for two beam energies. In the reaction $^{21}Ne + {}^{22}NaF$ at $E_{lab} = 2.1$ AGeV the K^+ cross section is $\sigma_{K^+} \simeq 23 \pm 8$ mb [30], and at $E_{lab} = 1$ AGeV one finds $\sigma_{K^+} \simeq 0.3 \pm 0.1$ mb for the $^{21}Ne + {}^{22}NaF$ reaction and $\sigma_{K^+} \simeq 41 \pm 7$ mb for the $^{197}Au + {}^{197}Au$ reaction, respectively [31]. From these experimental data, we find the K^- chemical potentials at the breakup time $\mu_K(t_o, E_{lab} = 2.1 \text{ AGeV}) \simeq -(2.6 \pm 0.2)m_\pi$ and $\mu_K(t_o, E_{lab} = 1 \text{ AGeV}) \simeq -(3.2 \pm 0.2)m_\pi$ for Ne data and $\simeq -(2.6 \pm 0.1)m_\pi$ for Au data. The breakup temperatures are extracted from [18] as 92 MeV at $E_{lab} = 2.1$ AGeV and 65 MeV at $E_{lab} = 1$ AGeV, respectively. In order to obtain the values $\mu_K(t_o, E_{lab})$ also for other collision energies we use the result of microscopical calculations [20], where it is shown that the logarithm $\lg \sigma_{K^+}(A, E_{lab})$ depends only weakly on the value E_{lab} within the energy interval 1 AGeV$\lesssim E_{lab} \lesssim$ 2 AGeV under consideration. This allows us to interpolate the dependence $\lg \sigma_{K^+}(A, E_{lab})$ in this energy interval by a square root function, i.e.,

$$\lg \left[\frac{\sigma_{K^+}(A, E_{lab})}{A^2} \right] = \left(a \frac{\sqrt{E_{lab}[GeV]} - 1}{\sqrt{2.1} - 1} + b \right). \tag{12}$$

We also interpolate here the $\sigma_{K^+}(A)$ dependence by the above mentioned A^2-scaling.

5 Fireball breakup and strange particle yield

According to our scenario the kaonic excitations evolve from their in-medium states to the free states within approximately the same collision stage $t_o - \tau_b/2 < t < t_o + \tau_b/2$

as the nucleons and pions do. Applying the sudden breakup model [15, 18] for the kaon momentum distribution one can derive the following relations

$$\begin{aligned}\frac{dN}{Vd^3k/(2\pi)^3} &= 2\omega_k\langle\Phi(t_0+\frac{\tau_b}{2})|\hat{\varphi}^*_{K^-}\hat{\varphi}_{K^-}|\Phi(t_0+\frac{\tau_b}{2})\rangle \\ &\simeq 2\omega_k\langle\Phi(t_0-\frac{\tau_b}{2})|\hat{\varphi}^*_{K^-}\hat{\varphi}_{K^-}|\Phi(t_0-\frac{\tau_b}{2})\rangle \\ &= 2i\omega_k\int_0^\infty \mathcal{D}^{-+}_{K^-}(t_0-\tau_b/2,t_0-\tau_b/2,\omega,k)\frac{d\omega}{2\pi},\end{aligned} \tag{13}$$

where $|\Phi\rangle$ is the state vector of the kaon sub–system, $\hat{\varphi}_{K^-}$ denotes the K^- field operator, and $\mathcal{D}^{-+}_{K^-}$ is the non-equilibrium K^- meson Green's function in the Wigner $4-(X,k)$ representation [32]. We assume here a homogeneous expansion, so that the Green's function does not depend on the spatial variable. Notice that the first two lines in eq. (13) relate the in-medium kaon spectrum to the free-streaming kaons. In this way we bridge over the complicated (and still unresolved) process of evolving in-medium quasi-particle excitations to real on-shell particles [33].

We suppose a quasi-equilibrium at $t = t_o - \tau_b/2$ and apply the equilibrium relation between the $\mathcal{D}^{-+}_{K^-}$ Green's function and the retarded Green's function $\mathcal{D}^R_{K^-}$ [27]

$$\mathcal{D}^{-+}_K(\omega,k) = 2i\frac{Im\mathcal{D}^R(\omega+\mu_K,k)}{\exp(\omega/T)-1}.$$

Then, in the quasi-particle approximation, i.e., $Im\Pi^R_{K^-}\to 0$, we have

$$\begin{aligned}\frac{dN}{d^3k/(2\pi)^3} &= -2\omega_k V_b\int_0^\infty\frac{d\omega}{2\pi}\frac{2Im\mathcal{D}^R_{K^-}(\omega+\mu_K,k)}{\exp(\omega/T_b)-1} \\ &\approx V_b\sum_{i=1}^{2}\Gamma_i(k)\exp\left(-\frac{\omega_i(k)}{T_b}+\frac{\mu_K}{T_b}\right).\end{aligned} \tag{14}$$

Here the sum is taken over the in-medium branches of kaonic excitations, and the factors $\Gamma_i(k)$ are given by eq. (5). The quantities V_b and μ_K stand for the fireball volume and the kaon chemical potential, respectively, at the breakup moment.

The breakup can be indeed considered as sudden for a given kaon of momentum k and energy ω in the medium if the breakup time τ_b is short compared with a typical time of the kaon absorbtion and compared with a typical time scale τ of the kaon transition from in-medium state to the vacuum state $\tau(\omega,k) = |\omega-\omega_k|^{-1}$.

In the presence of several branches in the excitation spectrum, the conditions of the breakup promptness have to be verified for every branch separately. Using an estimate of the breakup time [15, 18] $\tau_b \sim (1-2)/m_\pi$ we have $\tau_1 = \tau(\omega_1(k),k) \gg \tau_b$ for the upper in-medium branch of the K^- mesons, and $\tau_2 = \tau(\omega_2(k),k) < \tau_b$ for the low-lying branch. Thereby, for the kaons from the upper branch the breakup can be considered as rather fast, i.e., the K^- leaves the fireball with frozen in in-medium spectrum, whereas the kaons from the low-lying branch have enough time to leap to the vacuum states during

the breakup process. The latter contribution to the K^- yield is then determined by the vacuum dispersion law and by the chemical potential μ_2 which fixes the number of kaons on this low-lying branch just before breakup.

As result the invariant differential cross section of the K^- production renders

$$\omega_k \frac{d\sigma}{d^3k} = \frac{\sigma_{geom} V_b \omega_k}{(2\pi)^3} \times \left\{ \Gamma_1(k) \exp\left(-\frac{\omega_i(k)}{T_b} + \frac{\mu_K}{T_b} \right) + \exp\left(-\frac{\omega_k}{T_b} + \frac{\mu_2}{T_b} \right) \right\} \tag{15}$$

The total cross section of the neutral hyperon Λ, Σ° production can be estimated now as

$$\sigma_{\Lambda+\Sigma^\circ} = \sigma_{geom} V_b \left\{ \rho_\Lambda(\rho_b, T_b) + \frac{1}{3} \rho_\Sigma(\rho_b, T_b) \right\}. \tag{16}$$

Of course, these estimates are rather rough. Therefore we confront our developed model with experimental data to get some confidence of its reliability.

6 Results

Let us now compare the K^- yields, calculated within our scenario of strangeness production, with available experimental data. Unfortunately most of the data exist for forward angles, whereas our isotropical model is probably more appropriate for somewhat larger angles ($\theta_{c.m.} \sim 90^o$). However, some experiments [3] show that the K^- yield depends rather weakly on the production angle. This is in favour of our isotropy assumption.

Fig. 3 displays the invariant differential cross section of the K^- production for the reactions $^{28}Si + ^{28}Si$ and $^{21}Ne + ^{22}NaF$ at $E_{lab} = 2.1$ AGeV, and $^{58}Ni + ^{58}Ni$ at $E_{lab} = 1.85$ AGeV, calculated via eq. (15). One observes a good overall agreement of our in-medium strange particle production model with the experimental findings. The curves calculated with the free kaon spectrum, depicted also in Fig. 3 by dashed lines, lie below the experimental data (roughly a factor of 3). The same is seen in Fig. 4 for the collisions $^{28}Si + ^{28}Si$ at various lower bombarding energies. Although the uncertainties in the experimental cross sections of the K^+ production and the corresponding deviations of the chemical potentials of K^- mesons determine some interval for the values of the K^- cross sections, they do not change the relative positions of the calculated curves and the experimental points.

In Fig. 3 and 4 we have plotted also the results of calculations performed within our scenario but with the polarization operator of ref. [7], which includes only the s-wave KN interaction, leaving, therefore, out the Λ branch of kaonic excitations. The K^- yields are in this case somewhat smaller than those calculated with accounting for the p-wave interaction (i.e. accounting properly for the presence of the low-lying in-medium Λ branch). In spite of the deviations by a factor 1.5 for energies $E_{lab} \sim 2$ AGeV, both results are still within the experimental errors for the $Si + Si$ and $Ne + Na$ reactions.

For the $Ni + Ni$ reactions at $E_{lab} \sim 2$ AGeV and for $Si + Si$ at smaller beam energies these deviations increase up to a factor 3 at $E_{lab} = 1$ AGeV for $Si + Si$ within our fireball scenario. For $^{197}Au + ^{197}Au$ the deviations amount up to a factor of 5 at $E_{lab} = 1$ AGeV and rise up to a factor 20 at $E_{lab} = 0.5$ AGeV, see Fig. 5.

Thus the analysis of Figs. 3 - 5 shows that the in-medium effects become more pronounced in the deep subthreshold region at low beam energies, where the breakup temperature is lower than the difference of the in-medium kaon mass from the vacuum one. (A similar conclusion is put forward recently for K^+ yields [9].) Fig. 5 demonstrates also that due to the additional occupation factors (5) the spectra, which takes into account the in-medium kaon polarization, have slightly different slopes compared with those for the free kaons. Unfortunately, for such low energies K^- data are not yet measured.

Since the $FOPI$ collaboration at $GSI - SIS$ is going to measure the K^-, K^+ cross sections in $Ni + Ni$ reactions at $E_{lab} = 1.93$ AGeV we use our model to make some predictions. The corresponding breakup temperature is about 88 MeV. From the interpolation (12) the K^+ production cross section is found as to $\sigma_{K^+}(Ni, 1.93\text{AGeV}) \simeq 98$ mb. The corresponding K^- total cross section is consequently $\sigma_{K^-} \simeq 2$ mb and the momentum distribution is near to that depicted in Fig. 3 (curves A). Concerning the neutral hyperon production we predict from eq. (16) $\sigma_{\Lambda+\Sigma^0}(Ni, 1.93\text{AGeV}) \simeq 22$ mb, where Σ^0 particles contribute about 33%. Without any in-medium effects (i.e., keeping the $i = 1$ term in eq. (14) with $\Gamma_{K^*-}(k) = 1$ and $\omega_{K^*-}(k) = \sqrt{m_{K^*-} + k^2}$, where $m_{K^*-} \approx 6.4 m_\pi$ is the bare heavy kaon mass) we can estimate in the present fireball model the K^{*-} cross section as $\sigma_{K^*-}(Ni, 1.93\text{AGeV}) \simeq 3 \cdot 10^{-3}$ mb.

7 Summary

In summary we conclude that in-medium effects within our fireball scenario manifest themselves through an enhancement of the K^- yield in HIC when comparing with free kaons. The medium caused enhancement becomes more pronounced with decreasing beam energy and increasing atomic weight of the colliding nuclei. The differential cross sections calculated with s-wave kaon–nucleon interaction alone and with both s- and p- waves (as well as with some residual interaction taken into account) deviate by a factor 1.5 - 3 from each other. However, in view of the lack of precise data, as well as the absence of data for such heavy ions as Au, especially in the deep subthreshold range of beam energies ($\simeq 1$ AGeV), it is difficult to identify unambiguously the peculiarities in the in-medium kaon–nucleon interaction (such as the presence of the low–lying Λ branch in the kaon spectrum). For this, further detailed experiments with heavy ions at energies around 1 AGeV are desirable.

Acknowledgements: One of us (D.N.V.) acknowledges the hospitality and support of GSI, Darmstadt, and the Danish Natural Science Research Council for support of his visit at the Niels Bohr Institute. The research described in this publication was also made possible for him in part by Grant N3W000 from International Science Foundation. The work is supported in part by the BMFT grant 06DR666.

References

[1] A. Shor et al., Phys. Rev. Lett. **48** (1982) 1597.

[2] E. Barasch et al., Phys. Lett. **B161** (1985) 265.

[3] J. Carrol, Nucl. Phys. **A488** (1988) 203c.

[4] A. Shor et al., Phys. Rev. Lett. **63** (1989) 2192;
A. Shor, Phys. Lett. **B274** (1992) 11.

[5] A. Schröter et al., Z. Phys. A **350** (1994) 101.

[6] C.M. Ko, Phys. Lett. **B120** (1983) 294; **B138** (1984) 361;
H.W. Barz, H. Iwe, Phys. Lett. **B153** (1985) 217;
S.W. Huang, G.Q. Li, T. Maruyama, A. Faessler, Nucl. Phys. **A547** (1993) 653;
G.Q. Li, C.M. Ko, B.A. Li, Phys. Rev. Lett. **74** (1995) 235;
V. Koch, preprint SUNY-NTG 94-27 (1994).

[7] G.Q. Li, C.M. Ko, X.S. Fang, Phys. Lett. **B329** (1994) 149.

[8] J. Aichelin, C.M. Ko, Phys. Rev. Lett. **55** (1985) 2661;
C. Hartnack, J. Aichelin, H. Stöcker, W. Greiner, Phys. Rev. Lett. **72** (1994) 3767.

[9] G.Q. Li, C.M. Ko, Phys. Lett. **B349** (1995) 405.

[10] H. Stöcker, W. Greiner, Phys. Rep. **137** (1986) 277.

[11] P.J. Siemens, J.O. Rasmussen, Phys. Rev. Lett. **42** (1976) 880.

[12] B. Friedman , V.R. Pandharipande, Q.N. Usmani, Nucl. Phys. **A372** (1981) 483.

[13] D.N. Voskresensky, Yad. Fiz. **50** (1989) 1583 [Sov. J. Nucl. Phys. **50** (1989) 983].

[14] D.N. Voskresensky, A.V. Senatorov, Yad. Fiz. **53** (1991) 1521 [Sov. J. Nucl. Phys. **53** (1991) 935].

[15] A.V. Senatorov, D.N. Voskresensky, Dokl. Akad. Nauk. SSSR **303** (1988) 606 [Sov. Phys. Dokl. **303** (1988) 845]; Phys. Lett. **B219** (1989) 31.

[16] D.N. Voskresensky, O.V. Oreshkov, Yad. Fiz. **50** (1989) 1317[Sov. J. Nucl. Phys. **50** (1989) 820].

[17] D.N. Voskresensky, A.V. Senatorov, Yad. Fiz. **52** (1990) [Sov. J. Nucl. Phys. **52** (1990) 284]. 447;
D.N. Voskresensky, E.E. Kolomeitsev, Yad. Fiz. **56** (1993) 192 [Phys. At. Nucl. **56** (1993) 252]; Yad. Fiz. **58** (1994) 132 [Phys. At. Nucl. **58** (1995) 126].

[18] A.B. Migdal, E.E. Saperstein, M.A. Troitsky, D.N. Voskresensky, Phys. Rep. **192** (1990) 179;
D.N. Voskresensky, Nucl. Phys. **A555** (1993) 293.

[19] V.D. Toneev, H. Schulz, K.K. Gudima, G. Röpke, Sov. J. Part. Nucl. **17** (1986) 485;
B. Schürmann, W. Zwermann, R. Malfliet, Phys. Rep. **147** (1987) 1;
W. Cassing, V. Metag, U. Mosel, K. Niita, Phys. Rep. **188** (1990) 363;
V.N. Ruskikh, Yu.B. Ivanov, Nucl. Phys. **A543** (1992) 751;
A. Lang, W. Cassing, U. Mosel, K. Weber, Nucl. Phys. **A541** (1992) 507;
S.W. Huang, A. Faessler, G.Q. Li, R.K. Puri, E. Lehmann, D.T. Khoa, M.A. Matin, Phys. Lett. **B298** (1993) 41;
C. Hartnak, J. Jaenicke, L. Sehn, H. Stöcker, J. Aichelin, Nucl. Phys. **A580** (1994) 643;
X.S. Fang, C.M. Ko, L.Q. Li, Y.M. Zheng, Phys. Rev. **C49** (1994) R608.

[20] V.D. Toneev, K.K. Gudima, preprint GSI-93-52 (1993).

[21] S.A. Bass, M. Hofmann, C. Hartnack, H. Stöcker, W. Greiner, Phys. Lett. **B335** (1994) 289.

[22] H.W. Barz, L.P. Csernai, W. Greiner, Phys. Rev. **C26** (1982) 740.

[23] C. Greiner, P. Koch, H. Stöcker, Phys. Rev. Lett. **58** (1987) 1825;
C. Greiner, H. Stöcker, Phys. Rev. **D44** (1991) 3571.

[24] E.E. Kolomeitsev, D.N. Voskresensky, B. Kämpfer, Preprint FZR-94-40, Nucl. Phys. A (1995) in press; Proc. Int. Workshop XXIII on Gross Properties of Nuclei and Nuclear Excitations, (Eds.) H. Feldmeier, W. Nörenberg, Hirschegg, Austria, Jan. 16-21, 1995, p. 320

[25] G.E. Brown, C.H. Lee, M. Rho, V. Thorsson, Nucl. Phys. **A567** (1994) 937.

[26] M. Cubero, M. Schönhofen, H. Feldmeier, W. Nörenberg, Phys. Lett. **B201** (1988) 11.

[27] P. Danielewicz, Ann. Phys. (N.Y.) **152** (1984) 1628;
W. Boutermans, R. Malfliet, Phys. Rep. **198** (1990) 115.

[28] N.K. Glendenning, Astr. J. **293** (1985) 470.

[29] J.P. Bondorf, S.I.A. Garpman, J. Zimanyi, Nucl. Phys. **A296** (1978) 320.

[30] S. Schnetzer et al., Phys. Rev. **C40** (1989) 640.

[31] E. Grosse, Prog. Part. Nucl. Phys. **30** (1993) 89;
D. Miskoviec et al., Phys. Rev. Lett. **72** (1994) 3650.

[32] E.M. Lifshitz, L.P. Pitaevskii, Physical Kinetics, Pergamon Press, N.Y., 1981

[33] D.N. Voskresensky, D. Blaschke, G. Röpke, H. Schulz, preprint MPG-VT-UR 37/94, Rostock University (1994), Journ. Mod. Phys. **E4** (1995) in press.

Figure captions

Fig. 1: Spectrum of $K^-(\bar{K}^o)$ mesons (left panel (a)) and occupation factors $\Gamma_i(k)$ (right panel (b)) in isotopically symmetrical nuclear matter calculated with the in-medium Green's function (4) at the breakup density $\rho_b = 0.6\rho_o$ (solid lines) and at a certain initial density $\rho_m = 3\rho_o$ (dashed lines). The kaon branch $\omega_K(k)$ is labeled by 1, whereas the Λ branch $\omega_\Lambda(k)$ is labeled by 2. The dotted lines depict the free kaons ($\omega = \sqrt{m_K^2 + k^2}$) and the free Λ ($\omega = \sqrt{m_\Lambda^2 + k^2} - m_N$). Kaon frequency and momentum are displayed in pionic units.

Fig. 2: Time evolution of the relative weights of the negatively strange particles $c_K = c_{K^-} = c_{\bar{K}^o}$, c_Λ and c_Σ for $K^-(\bar{K}^o)$, Λ and Σ, respectively, calculated with the in-medium kaon spectrum (solid lines) and the free kaon spectrum (dashed lines). Initial and final temperatures (densities) are equal to $T_m = 133$ MeV ($\rho_m = 3\rho_o$) and $T_b = 92$ MeV ($\rho_b = 0.6\rho_o$) corresponding (in accordance with refs. [13, 18]) to the beam energy $E_{lab} = 2.1$ AGeV.

Fig. 3: The logarithm of the invariant differential cross section $\omega_k \frac{d\sigma_{K^-}}{d^3k} \left[\frac{mb}{GeV^2}\right]$ of K^- production as a function of the center-of-mass kinetic energy of kaons calculated via eq. (15) for $^{58}Ni + ^{58}Ni$ collisions at $E_{lab} = 1.85$ AGeV (curves A) and for $^{28}Si + ^{28}Si$ (B) and $^{21}Ne + ^{22}NaF$ (C) collisions at $E_{lab} = 2.1$ AGeV. Dashed curves are calculated with the free kaon spectrum, whereas dash-dotted curves employ the kaon polarization operator of ref. [7], which includes only the s-wave KN interaction. Experimental data are from ref. [5] for Ni, [2, 3] for Si and [4] for Ne.

Fig. 4: The same as in Fig. 3, but for $^{28}Si + ^{28}Si$ collisions at collision energies $E_{lab} = 1.65$ AGeV (curves A), 1.4 AGeV (B) and 1.16 AGeV (C). The experimental data are from refs. [3, 4].

Fig. 5: The same as in Fig. 3, but for $^{197}Au + ^{197}Au$ reactions at $E_{lab} = 1$ AGeV (curves A) and at $E_{lab} = 0.5$ AGeV (B).

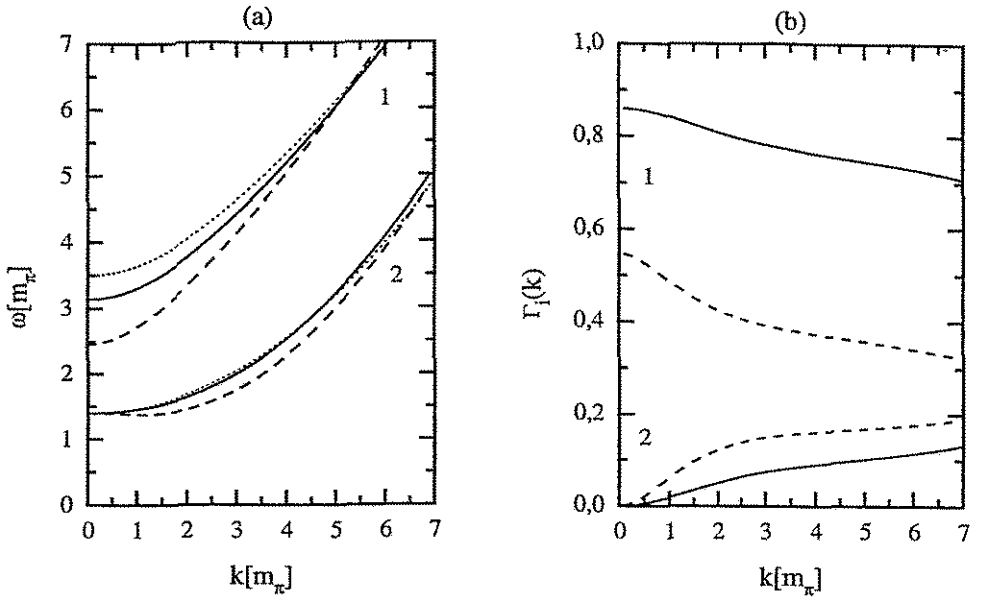

Figure 1: Spectrum of $K^-(\bar{K}^o)$ mesons (left panel (a)) and occupation factors $\Gamma_i(k)$ (right panel (b)) in isotopically symmetrical nuclear matter calculated with the in-medium Green's function (4) at the breakup density $\rho_b = 0.6\rho_o$ (solid lines) and at a certain initial density $\rho_m = 3\rho_o$ (dashed lines). The kaon branch $\omega_K(k)$ is labeled by 1, whereas the Λ branch $\omega_\Lambda(k)$ is labeled by 2. The dotted lines depict the free kaons ($\omega = \sqrt{m_K^2 + k^2}$) and the free Λ ($\omega = \sqrt{m_\Lambda^2 + k^2} - m_N$). Kaon frequency and momentum are displayed in pionic units.

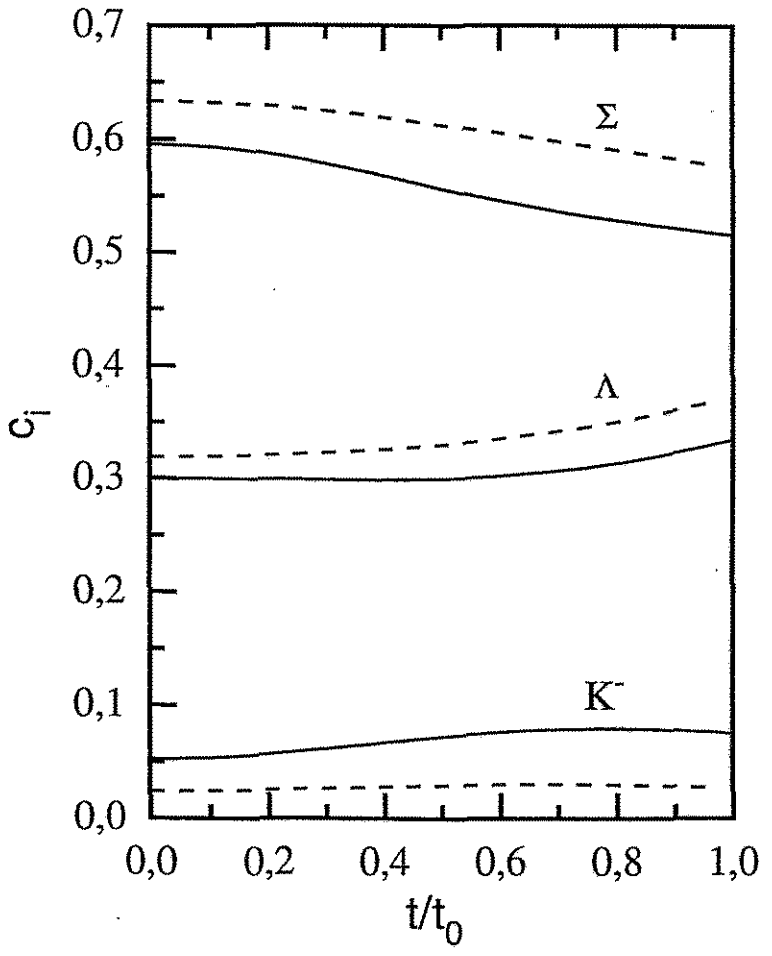

Figure 2: Time evolution of the relative weights of the negatively strange particles $c_K = c_{K^-} = c_{\bar{K}^o}$, c_Λ and c_Σ for $K^-(\bar{K}^o)$, Λ and Σ, respectively, calculated with the in-medium kaon spectrum (solid lines) and the free kaon spectrum (dashed lines). Initial and final temperatures (densities) are equal to $T_m = 133$ MeV ($\rho_m = 3\rho_o$) and $T_b = 92$ MeV ($\rho_b = 0.6\rho_o$) corresponding (in accordance with refs. [13, 18]) to the beam energy $E_{lab} = 2.1$ AGeV.

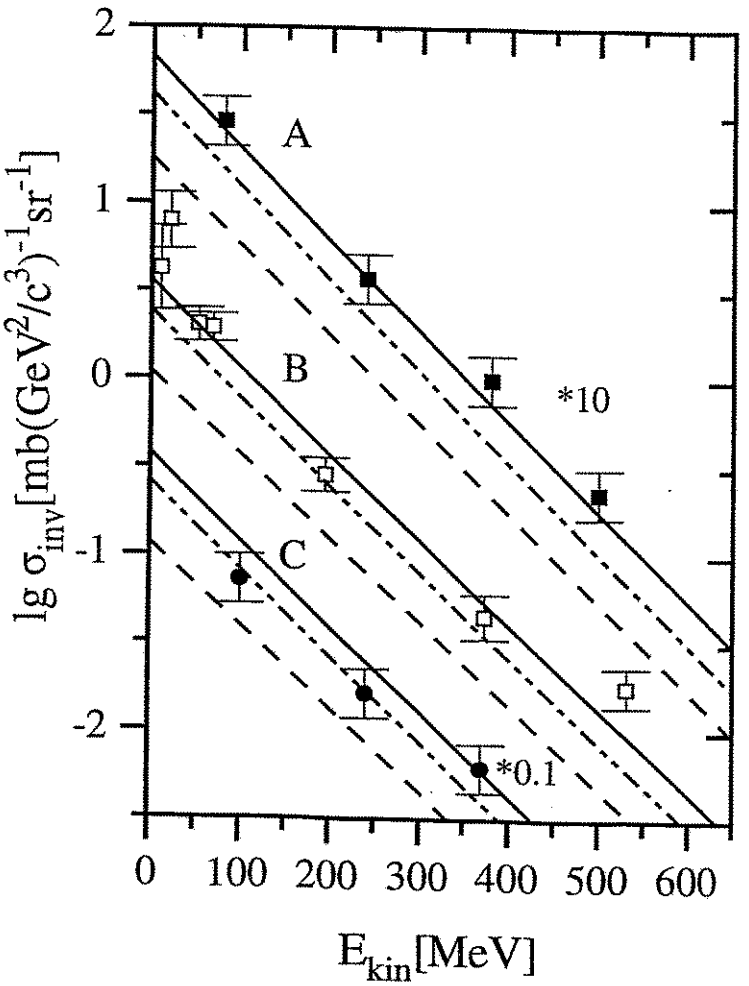

Figure 3: The logarithm of the invariant differential cross section $\omega_k \frac{d\sigma_{K^-}}{d^3k} \left[\frac{mb}{GeV^2}\right]$ of K^- production as a function of the center-of-mass kinetic energy of kaons calculated via eq. (15) for $^{58}Ni + ^{58}Ni$ collisions at $E_{lab} = 1.85$ AGeV (curves A) and for $^{28}Si + ^{28}Si$ (B) and $^{21}Ne + ^{22}NaF$ (C) collisions at $E_{lab} = 2.1$ AGeV. Dashed curves are calculated with the free kaon spectrum, whereas dash-dotted curves employ the kaon polarization operator of ref. [7], which includes only the s-wave KN interaction. Experimental data are from ref. [5] for Ni, [2, 3] for Si and [4] for Ne.

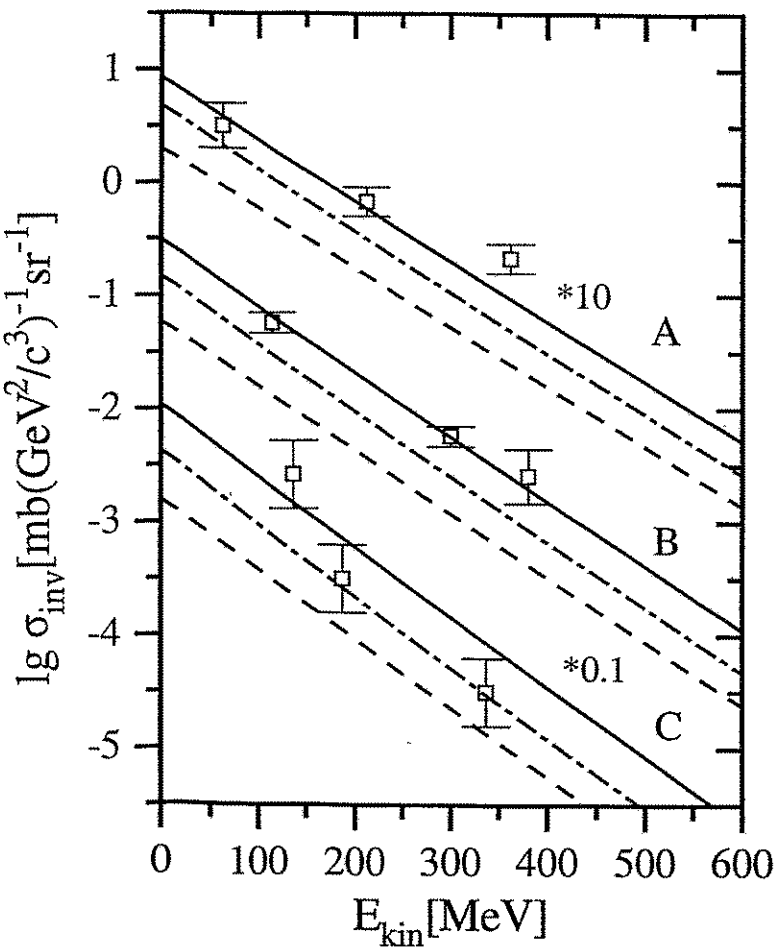

Figure 4: The same as in Fig. 3, but for $^{28}Si + ^{28}Si$ collisions at collision energies E_{lab} = 1.65 AGeV (curves A), 1.4 AGeV (B) and 1.16 AGeV (C). The experimental data are from refs. [3, 4].

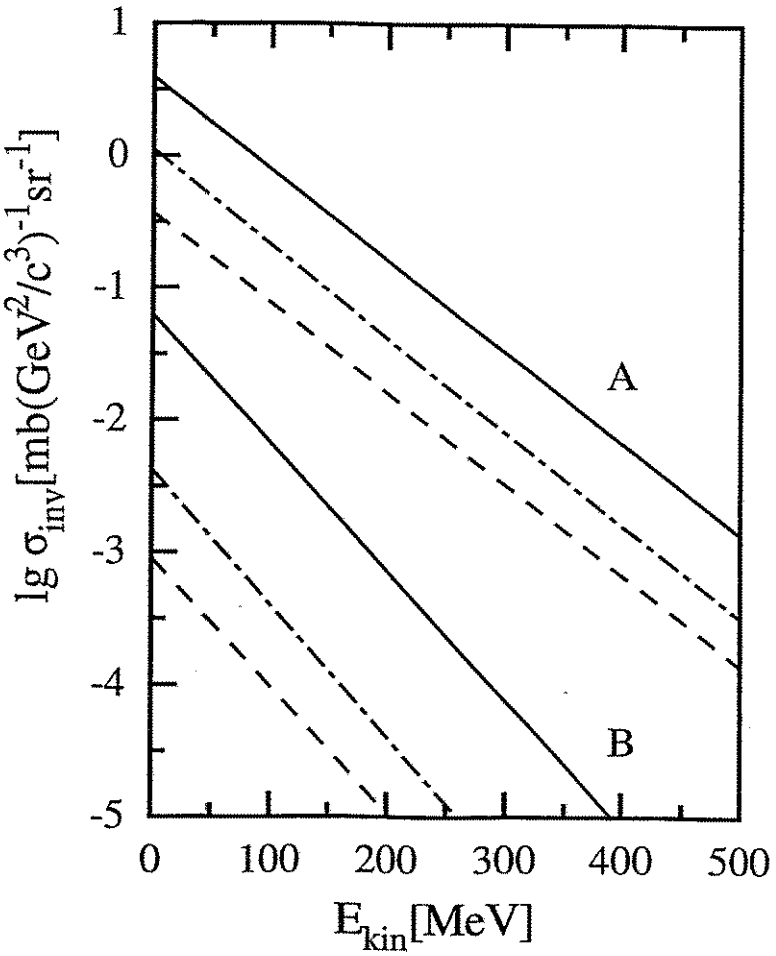

Figure 5: The same as in Fig. 3, but for $^{197}Au+^{197}Au$ reactions at $E_{lab} = 1$ AGeV (curves A) and at $E_{lab} = 0.5$ AGeV (B).